Neurobiology of Disease 216 (2025) 107140

Contents lists available at ScienceDirect

Neurobiology of Disease

journal homepage: www.elsevier.com/locate/ynbdi

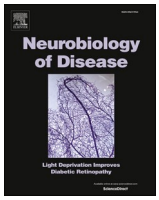

APOE4 carriership status influences [^{11}C]PiB white matter retention in cognitively healthy older adults

Claudia Tato-Fernández [a,b,*], Laura L. Ekblad [a,b,c], Marco Bucci [a,b,d], Jouni Tuisku [a,b], Riitta Parkkola [e], Semi Helin [a], Juha O. Rinne [a,b,f], Anniina Snellman [a,b]

[a] Turku PET Centre, University of Turku, Turku, Finland
[b] Turku PET Centre, Turku University Hospital, Wellbeing Services of Southwest Finland, Turku, Finland
[c] Department of Geriatric Medicine, University of Turku and Turku University Hospital, Wellbeing Services County of Southwestern Finland, Turku, Finland
[d] Department of Neurobiology, Care Sciences and Society, Centre for Alzheimer Research, Division of Clinical Geriatrics, Karolinska Institutet, SE-14183 Stockholm, Sweden
[e] Department of Radiology, University of Turku and Turku University Hospital, Turku, Finland
[f] InFLAMES Research Flagship Center, University of Turku, Turku, Finland

ARTICLE INFO

Keywords:
^{11}C-labelled Pittsburgh compound B
APOE
ApolipoproteinE
Myelin
PET
DTI
NAWM
WMHs

ABSTRACT

Purpose: The objective of this study was to assess whether *APOE4* carriership status affects white matter (WM) [^{11}C]PiB positron emission tomography (PET) retention in cognitively healthy older adults, as a potential indicator of myelin integrity.
Methods: We explored WM [^{11}C]PiB retention of 101 participants (non-carriers, $n = 40$; *APOE3/4* carriers, n = 40; *APOE4/4* carriers, $n = 21$) and its association with fractional anisotropy, a diffusion tensor imaging measure reflecting WM microstructure. WM [^{11}C]PiB retention was assessed in voxel-wise analysis and within normal-appearing white matter (NAWM) and white matter hyperintensities (WMHs) as regions-of-interest.
Results: [^{11}C]PiB retention was lower in WMHs than NAWM ($p_{t\text{-test}} < 0.001$). In NAWM, *APOE4/4* and *APOE3/4* carriers showed reduced [^{11}C]PiB retention compared to non-carriers ($p_{ANCOVA} = 0.040$, among all groups), while there were no significant differences in [^{11}C]PiB retention within regions of WMHs ($p_{ANCOVA} = 0.11$). *APOE4/4* carriers had lower WM [^{11}C]PiB retention than non-carriers in voxel-wise analysis ($p_{FWE} < 0.05$). WM [^{11}C]PiB retention was not associated with fractional anisotropy, suggesting different pathological pathways.
Conclusion: A decrease in NAWM [^{11}C]PiB retention is suggestive of myelin damage prior to the onset of cognitive decline in *APOE4* homozygotes.

1. Introduction

Alzheimer's disease (AD) is the most common cause for dementia and a major cause of disability (Nichols et al., 2022). The most important genetic risk factor for AD is *APOE* ε4 (*APOE4*) carriership and *APOE4/4* homozygosity has been suggested to represent a genetic form of AD (Fortea et al., 2024). Demyelination, *i.e.* the disruption of the cholesterol-rich myelin sheath that encircles axons, is a feature seen in neurological disorders, including AD (Bouhrara et al., 2018; Dean et al., 2017). *APOE4* could increase the risk for AD *via* deficits in oligodendrocytic function that result in demyelination (Bartzokis, 2011; Blanchard et al., 2022). The hallmark pathological sign of AD, cortical beta-amyloid (Aβ) plaques, can be detected *in vivo* with positron emission tomography (PET). Recent studies have repurposed amyloid-PET tracers to assess myelin integrity in the AD continuum (Moscoso et al., 2022; Rubinski et al., 2023), but it has not yet been evaluated whether Thioflavin T analog ^{11}C-labelled Pittsburgh compound B ([^{11}C]PiB) can be utilized to detect white matter (WM) changes in cognitively unimpaired *APOE4/4* homozygotes, who are at risk for developing clinical AD.

[^{11}C]PiB binds with high affinity to the beta-sheet structure of Aβ plaques (Klunk et al., 2004) and is used for *in vivo* quantification of Aβ burden, along with several ^{18}F-labelled tracers, including [^{18}F]Florbetapir, [^{18}F]Florbetaben and [^{18}F]Flutemetamol. Amyloid-PET tracers also show retention in the WM of healthy individuals and patients with AD (Klunk et al., 2004), with inter-tracer differences pointing that ^{18}F-labelled tracers have higher WM retention than [^{11}C]PiB (Bao et al.,

* Corresponding author at: Turku PET Centre, Kiinamyllynkatu 4-8, 20521 Turku, Finland.
E-mail address: claudia.tatofernandez@varha.fi (C. Tato-Fernández).

https://doi.org/10.1016/j.nbd.2025.107140
Received 18 August 2025; Received in revised form 8 October 2025; Accepted 11 October 2025
Available online 13 October 2025

2017; Landau et al., 2014). Fluorinated ligands have higher lipophilicity, which might explain their higher WM retention (Kepe et al., 2013). The topographic binding distributions of certain amyloid-PET tracers are comparable in grey matter, as has been shown with [^{18}F]Flutemetamol and [^{11}C]PiB (Zeydan et al., 2022); however, [^{18}F]Flutemetamol shows higher retention than [^{11}C]PiB in subcortical WM, whereas WM retention was comparable between [^{18}F]Florbetapir and [^{11}C]PiB (Landau et al., 2014). The WM binding of amyloid-PET tracers was considered non-specific, but several studies have suggested that these tracers additionally have an affinity for myelin (Pietroboni et al., 2022; Stankoff et al., 2011; Zeydan et al., 2022; Zhang et al., 2021a). [^{11}C]PiB labels WM *in vitro* and in human postmortem tissue (Stankoff et al., 2011), although the robustness of this finding is unclear (Fodero-Tavoletti et al., 2009). In patients with multiple sclerosis, [^{11}C]PiB retention is reduced in regions of white matter hyperintensities (WMHs) compared to normal-appearing white matter (NAWM), suggesting that this tracer can non-invasively detect myelin lesions *in vivo* (Campanholo et al., 2022; Stankoff et al., 2011). Myelin basic protein (MBP) is the major protein component of myelin. It has been postulated that MBP has a core element of beta-sheet, where [^{11}C]PiB is thought to bind (Stankoff et al., 2011). When myelin is damaged, it loses its beta-sheet structure, which could result in reduced amyloid-PET tracer binding (van der Weijden et al., 2023). However, amyloid-PET tracers might interact with targets that share similar molecular structures, affecting their specificity, and [^{11}C]PiB retention could be influenced by sulfotransferase activity, hydrophobic interactions or tissue-specific kinetics (Kepe et al., 2013; Surmak et al., 2020).

A [^{18}F]Florbetapir PET imaging study showed that patients with AD show lower tracer retention than cognitively healthy controls in the NAWM (Moscoso et al., 2022), suggesting that [^{18}F]Florbetapir PET could potentially be a more sensitive method for detecting demyelination than fluid-attenuated inversion recovery (FLAIR) magnetic resonance imaging (MRI), that is traditionally used to detect WMHs. In the context of AD, a decrease in [^{18}F]Florbetapir retention in WM is associated with longitudinal cognitive decline and faster rate of tau accumulation, the latter exacerbated by the *APOE4* allele (Rubinski et al., 2023). Preliminary evidence suggests that [^{11}C]PiB retention could be a marker of WM damage in AD (de Faria et al., 2019). However, these findings should be interpreted with caution, since a reduction in WM tracer retention might be caused by processes different than demyelination (Ottoy et al., 2023). Moreover, the pathology of WMHs is heterogenous and they might be driven by processes other than demyelination, including neurodegeneration and vessel amyloidosis (Shirzadi et al., 2023).

Diffusion tensor imaging (DTI) is frequently used to assess WM tissue microstructure from the MRI signal (Basser and Pierpaoli, 1996). Parameters derived from DTI, including fractional anisotropy (FA), can detect early neurodegeneration in patients with AD (Teipel et al., 2010). Several studies have reported WM impairment in *APOE4* carriers using DTI (Dowell et al., 2013; Gold et al., 2010; Tato-Fernández et al., 2024). Moreover, previous investigations have found a link between lower DTI-FA and reduced [^{18}F]Florbetapir retention in the WM (Moscoso et al., 2022; Ottoy et al., 2023), but DTI-FA is primarily an indicator of tissue microstructure (Basser and Pierpaoli, 1996).

Following the notion that [^{11}C]PiB binds to myelin, we aimed to investigate whether cognitively healthy older adults who carry one or two *APOE4* alleles, and are thus at risk for developing clinical AD, show reduced [^{11}C]PiB retention in NAWM and in regions of WMHs, compared to cognitively healthy non-carriers. Moreover, to enhance the interpretability of our findings, we explored the association between [^{11}C]PiB retention and tissue microstructure, measured with DTI-FA, in the cerebral WM.

2. Methods

2.1. Participants

The present study includes data from 101 cognitively healthy individuals (MMSE $\geq$ 24, CERAD neuropsychological total score (Chandler et al., 2005) > 62) aged 65–85 years, from two separate cohorts recruited at Turku PET Centre (Cohort 1: ASIC-E4, n = 63 (Snellman et al., 2022); Cohort 2: CIRI-5Y, n = 46 (Pietilä et al., 2024) (Fig. 1). Participants with one [^{11}C]PiB PET scan, one T1-weighted (T1w) and one FLAIR MRI scan available were included in this study. These individuals had *APOE2/3* (n = 5), *APOE3/3* (n = 35), *APOE3/4* (n = 40) or *APOE4/4* (n = 21) genotypes. *APOE2/3* and *APOE3/3* carriers showed no significant differences in WM [^{11}C]PiB retention and were pooled together as a non-carrier group (n = 40). Details regarding recruitment and *APOE* genotyping have been previously reported for both cohorts (Ekblad et al., 2018; Pietilä et al., 2024; Snellman et al., 2022). 98 of the participants additionally had a DTI scan available. Exclusion criteria were MMSE < 24, CERAD neuropsychological total score < 62, neurological or psychiatric diseases, or contraindications for MRI and PET imaging. After a visual quality control, two subjects were excluded from the study sample because they had large ventricles that interfered with inter-modal registration.

The ASIC-E4 and CIRI-5Y studies were approved by the ethics committee of the Hospital District of Southwest Finland. The studies were conducted in accordance with the Declaration of Helsinki. Participants signed a written informed consent.

2.2. Image acquisition

MRI data were acquired either with Philips Ingenia 3.0 T systems (Philips Healthcare, Amsterdam, the Netherlands, n = 22) or Philips Ingenuity 3.0 T TF PET-MR (Philips Healthcare, Amsterdam, the Netherlands, n = 79) at Turku PET Centre. T1w sequences, T2w FLAIR sequences and DTI sequences with opposing phase-encoding polarities were acquired for each participant (TR = 6700 ms, TE = 120 ms, 2 × 2 × 2 mm voxels, 80 axial slices, slice thickness = 2 mm, no slice gap, field of view = 256 × 256 mm^2, flip angle = 90, b-val = 1000 s/mm^2). Full imaging protocols are available in previous publications (Ekblad et al., 2018; Pietilä et al., 2024; Snellman et al., 2022; Tato-Fernández et al., 2024). MRI scans were reviewed by a neuroradiologist to exclude the presence of brain abnormalities.

PET data were acquired with High Resolution Research Tomograph (HRRT, Siemens Medical Solutions, Knoxville, TN). The spatial resolution for this scanner is 2.5 mm. PET images were acquired for 50 min, 40 min after injection of 250–500 MBq of [^{11}C]PiB. Each acquisition was followed by a 6 min transmission scan using a ^{137}Cs point source for attenuation correction. List-mode data was histogrammed into 8 time frames and reconstructed with 3D ordinary Poisson ordered subset expectation maximization algorithm (OP-OSEM3D) with 16 subsets and 8 iterations and a voxel size of 1.22 × 1.22 × 1.22 mm.

2.3. [^{11}C]PiB PET analysis

T1w MRI scans were processed with FreeSurfer (v. 7.2.0). To separately examine tracer retention in NAWM and WMHs, binary WMHs masks were first obtained from FLAIR images with an automatic cNeuroimage analysis tool (Combinostics Oy, Tampere, Finland) that used an adapted version of methods previously described (Koikkalainen et al., 2016). The same tool was used to estimate Computed Fazekas score. In line with previous studies (Moscoso et al., 2022; Ottoy et al., 2023; Rubinski et al., 2023), we i) filtered out lesion clusters with fewer than 26 voxels to minimize contamination from surrounding NAWM, ii) co-registered WMHs masks with T1w images and combined them with a binary WM tissue segmentation to create WM masks, thus ensuring that hypointense WM regions were not misclassified, iii) generated a

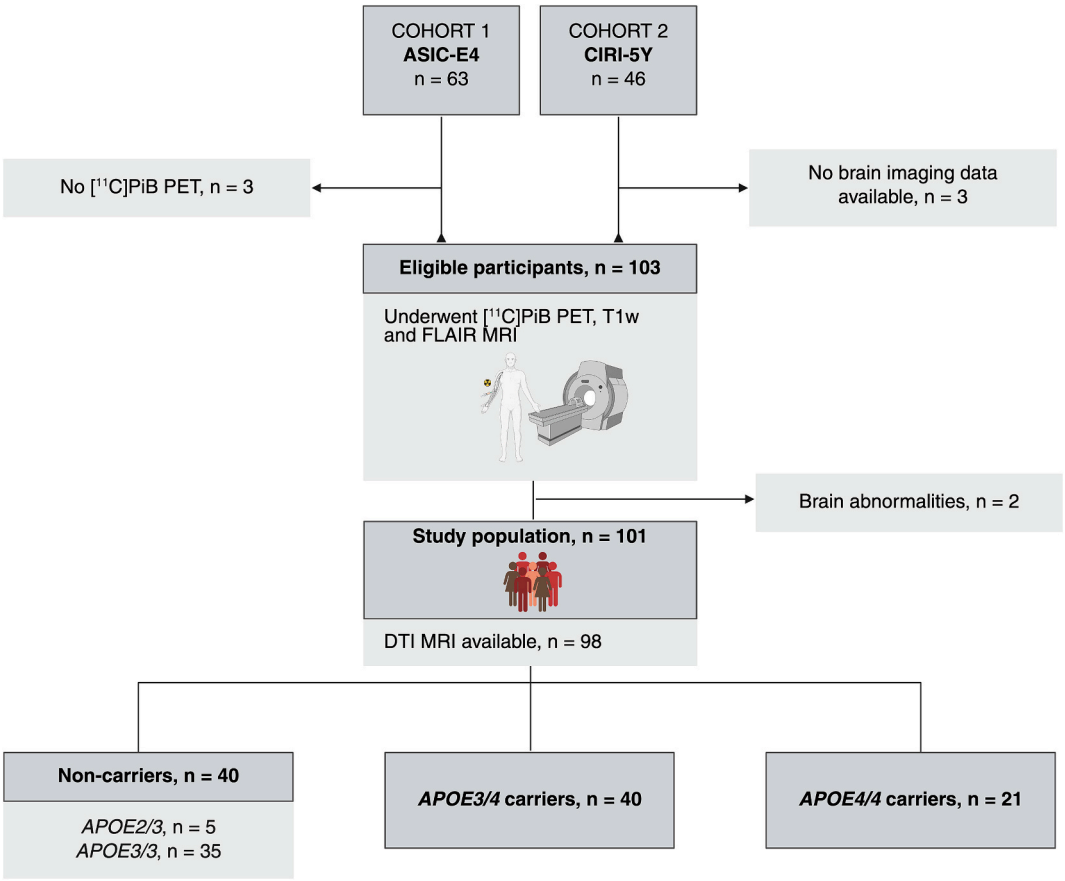

Fig. 1. Study flowchart. Out of the 103 eligible participants for the study, two were excluded after examining their brain images, rendering a total study population of 101 cognitively healthy individuals. In 98 cases, a DTI scan was available. https://BioRender.com/j77q867 DTI = diffusion tensor imaging, FLAIR = fluid-attenuated inversion recovery, MRI = magnetic resonance imaging, PET = positron emission tomography.

standard cerebral mask in Montreal Neurological Institute (MNI) space and warped the mask to each subject's native space to remove the cerebellum and brainstem from analysis, and iv) eroded WM masks to exclude voxels within 2 mm from cortical regions to minimize partial volume effects (PVEs). After processing the masks, all participants showed at least some WMHs. Lastly, NAWM masks were generated by subtracting WMHs from the WM masks.

PET images were processed using an automated pipeline (Karjalainen et al., 2020) built on MATLAB (vR2021b) which uses functions from SPM12 and FreeSurfer. This pipeline performs co-registration of a T1w scan to PET native space and region-of-interest (ROI) parcellation. Cerebellar grey matter was chosen as reference region to avoid circular analyses and it was corrected to minimize spill-over effects. Since previous studies reported that dynamic quantification and semi-quantitative methods have comparable accuracy when assessing Aβ load and demyelination (Carotenuto et al., 2020; Lopresti et al., 2005), [^{11}C]PiB retention was quantified as standardized uptake value ratios (SUVRs) for the 50–70 min time window within eroded WM, NAWM and WMH. A volume-weighted composite ROI was used to quantify cortical SUVRs, based on regions where cortical Aβ first appears in the AD continuum (Grothe et al., 2017), including prefrontal cortex, parietal cortex, anterior cingulum, posterior cingulum, precuneus and lateral temporal cortex. Parametric images were normalized and smoothed (8 mm) for whole-brain pairwise comparisons.

2.4. DTI analysis

DTI scans were corrected for subject motion, susceptibility- and eddy-current-induced distortions using the FMRIB Software Library v6.0.1 (Smith et al., 2004). Images were skull-stripped (Smith, 2002) and the tensor model was fit at each voxel. FA maps were thresholded at 0.2 to correct for PVEs and co-registered to T1w scans. The inverse transformation was applied to the eroded WM, NAWM and WMHs masks to estimate average DTI-FA within these ROIs.

2.5. Statistical analysis

Regional statistical analysis and data visualization were carried out with R v4.3.1 and Rstudio v2023.12.1+402. Normality of the distributions was assessed visually from the histograms. Demographic variables are presented as means (standard deviation) for normally distributed variables, or median (interquartile range) for non-normally distributed variables. Differences among *APOE* genotypes were assessed with one-way ANOVA (continuous variables, normally distributed), Kruskal-Wallis test (continuous variables, non-normally distributed), or χ^2 test (categorical variables). Significance was set at $p < 0.05$ (two-tailed). Pairwise comparisons were carried out with *post hoc* Tukey's honest significance test or Dunn's test in the case of global significant differences ($p < 0.05$). Normality of the residuals was verified with the histograms and homogeneity of variances with Levene's test ($p > 0.05$).

[^{11}C]PiB SUVRs were compared within a composite cortical ROI, NAWM and WMHs across all subjects with a paired *t*-test or Wilcoxon rank sum test. DTI-FA was compared between NAWM and WMHs across all subjects with Wilcoxon rank sum test. As previously reported (Moscoso et al., 2022), we verified that [^{11}C]PiB retention in WM is highly correlated with global cortical [^{11}C]PiB SUVR ($r_s = 0.73$, $p < 0.001$, Fig. 2). Therefore, we corrected our subsequent analyses for global cortical [^{11}C]PiB SUVR. WMH volumes were normalized by the

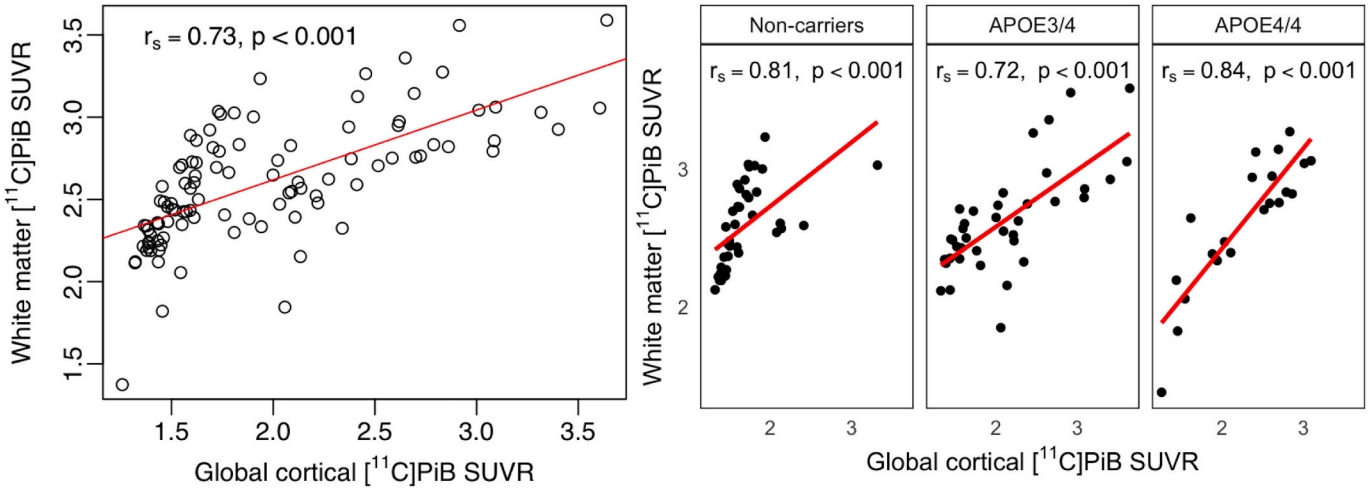

Fig. 2. Scatterplot showing Spearman's correlation (r_s) coefficient and its corresponding *p*-value between white matter and global cortical [^{11}C]PiB standardized uptake value ratio (SUVR) in the total study population (left) and stratified by *APOE* genotype (right).

total intracranial volume (ICV) and included as a covariate (Ottoy et al., 2023). Given that sex has a known effect on WMH load (Fatemi et al., 2018), we additionally tested for differences in normalized WMH volume based on sex.

Type 1 ANCOVA (Fox, 2008), adjusted for global cortical [^{11}C]PiB SUVR, age, sex and WMH volumes, was used to compare NAWM SUVR among the three *APOE* groups. Pairwise comparisons were carried out with Tukey's honest significance difference (HSD) test in the case of global significant differences ($p_{ANCOVA} < 0.05$). Voxel-wise comparisons were carried out in SPM12 within the WM using ANCOVA, with sex, age, global cortical [^{11}C]PiB SUVR and WMH volumes as covariates. Whole brain analyses were considered significant at $p < 0.05$, family-wise error (FWE) corrected for multiple comparisons.

Next, we assessed the correlation between [^{11}C]PiB SUVRs and tissue microstructure, estimated as DTI-FA, within regions of NAWM and WMHs in the whole study sample. After visual inspection of the scatterplots, we tested for monotonic relationships with Spearman's coefficient (r_s). If a significant correlation was found ($p < 0.05$), independent associations were further examined with linear regression, including global cortical [^{11}C]PiB SUVR, age, sex and WMH volumes as regressors.

For sensitivity analyses, we repeated our main analysis while excluding individuals with low WMHs ($n = 19$), defined as WMH volume < 1 cm^3 (Ottoy et al., 2023), to ensure that the results were not driven exclusively by these individuals, who are likely more vulnerable to PVEs from adjacent tissue.

3. Results

3.1. Study population

Table 1 shows the distribution of demographic variables in the total study population and stratified by *APOE* genotype. This study included 101 healthy volunteers (mean age = 71.3, standard deviation = 5.35), out of which 59.4% were females. Non-carriers, *APOE3/4* and *APOE4/4* did not significantly differ in terms of age, sex, education or WMH volumes. Global cortical SUVR increased in a gene dose-dependent way ($p_{Kruskal\text{-}Wallis} < 0.001$), with non-carriers showing lower retention than *APOE3/4* carriers ($p_{Dunn} = 0.0044$) and *APOE4/4* carriers ($p_{Dunn} < 0.001$). The groups did not significantly differ in CERAD total score ($p_{Kruskal\text{-}Wallis} = 0.73$), but there were significant differences in MMSE score ($p_{Kruskal\text{-}Wallis} = 0.047$). *APOE4/4* carriers had slightly lower MMSE score than non-carriers ($p_{Dunn} = 0.042$).

3.2. Interactions by sex

Females had higher WMH volumes than males ($p_{Kruskal\text{-}Wallis} = 0.017$). Sex did not have a significant effect on [^{11}C]PiB NAWM SUVR ($T = 1.89$, $p = 0.061$), nor [^{11}C]PiB WMH SUVR ($T = 1.92$, $p = 0.058$). When we included age as a covariate, the effect of sex on [^{11}C]PiB NAWM and WMH SUVR attenuated (F[1, 98] = 1.40, $p_{ANCOVA} = 0.24$, and F[1, 98] = 2.44, $p_{ANCOVA} = 0.12$, respectively).

Table 1
Demographic characteristics of the total study population and the three *APOE* groups.

	Total population	Non-carriers	*APOE3/4*	*APOE4/4*	p-value
N	101	40	40	21	
Age (years), mean (SD)	71.3 (5.35)	72.4 (4.96)	71.4 (5.24)	69.0 (5.45)	0.092
Sex (M/F), n	41/60	19/21	15/25	7/14	0.49
Education, n (%)					
Primary school	30 (29.7 %)	12 (33.3 %)	11 (27.5 %)	7 (30 %)	
Middle school	26 (25.7 %)	10 (28.6 %)	10 (25 %)	6 (25 %)	0.77
High school	25 (24.7 %)	11 (28.6 %)	8 (20 %)	6 (27.5 %)	
College or university	20 (19.8 %)	7 (9.52 %)	11 (27.5 %)	2 (17.5 %)	
BMI (kg/m^2), mean (SD)	26.9 (4.31)	27.8 (4.12)	26.3 (3.60)	26.5 (4.96)	0.24
MMSE, median (IQR)	29 (27–30)	29 (27–30)	28.5 (27.8–30)	28 (26–29)*	**0.047**
CERAD total score, median (IQR)	86 (79–92)	86.5 (78.8–92.3)	85.5 (81–91.3)	83 (76.5–91.3)	0.73
WMH volume (cm^3), median (IQR)	2.65 (1.43–5.51)	2.48 (1.23–6.17)	2.86 (1.39–4.43)	2.91 (1.67–6.14)	0.76
Computed Fazekas score (0–3), median (IQR)	0.96 (0–1.51)	0.74 (0–1.45)	0.98 (0–1.39)	0.96 (0–1.7)	0.63
Global cortical PiB retention (SUVR), median (IQR)	1.74 (1.48–2.34)	1.59 (1.44–1.75)	2.01 (1.55–2.40)**	2.42 (1.88–2.70)***	**0.00029**

The p-value refers to overall difference among the groups; statistical significance in relation to non-carriers is shown with star symbols (* $p < 0.05$, ** $p < 0.01$, *** $p < 0.001$). BMI = body-mass index, SD = standard deviation, WMH = white matter hyperintensity, MMSE = Mini-Mental State Examination, CERAD = Consortium to Establish a Registry for Alzheimer's Disease.

3.3. Analysis of NAWM and WMHs

In the total study population, we found significantly lower [^{11}C]PiB SUVRs ($p_{t\text{-test}} < 0.001$, Cohen's D = 1.00; Fig. 3A) and DTI-FA values ($p_{Wilcoxon} < 0.001$, Cohen's D = 2.92; Fig. 3B) in regions of WMHs, compared to NAWM. Global cortical [^{11}C]PiB SUVR was lower than [^{11}C]PiB NAWM SUVR ($p_{Wilcoxon} < 0.001$, Cohen's D = −1.34, Fig. 3A) and WMHs SUVR ($p_{Wilcoxon} < 0.001$, Cohen's D = −0.63, Fig. 3A).

Group comparisons among the three *APOE* groups evidenced statistically significant differences in [^{11}C]PiB SUVRs within NAWM (F[2, 94] = 3.34, 95 % CI [0.0017, 1.00], $p_{ANCOVA} = 0.040$, Fig. 4) in the fully adjusted model. Tukey's HSD test showed that *APOE4/4* carriers had numerically lower SUVR in NAWM, compared to non-carriers, at borderline significance level (95 % CI: [−0.39, 0.0013], $p_{Tukey} = 0.052$, Fig. 4), and *APOE3/4* carriers similarly showed numerically lower NAWM SUVR than non-carriers, though this was a non-significant trend (95 % CI: [−0.28, 0.015], $p_{Tukey} = 0.087$, Fig. 4). There were no significant differences between *APOE4/4* and *APOE3/4* carriers in NAWM [^{11}C]PiB SUVR (95 % CI: [−0.23, 0.11], $p_{Tukey} = 0.68$, Fig. 4). Our groups did not statistically differ in [^{11}C]PiB SUVR within regions of WMHs (F[2, 94] = 2.22, 95 % CI [0.00, 1.00], $p_{ANCOVA} = 0.11$, Fig. 4). Sequential results are available in Tables A.1 and A.2.

Similarly, our whole-brain analysis revealed a cluster in the right cerebral WM adjacent to the right cuneus where *APOE4/4* carriers exhibited significantly lower [^{11}C]PiB retention compared to non-carriers (cluster peak at 9 × -80 × 26, Broadmann area 18, size 173 voxels, $p_{FWE} < 0.05$, adjusted for sex, age, global cortical [^{11}C]PiB SUVR and WMH volumes) (Fig. 5). There were no significant WM clusters

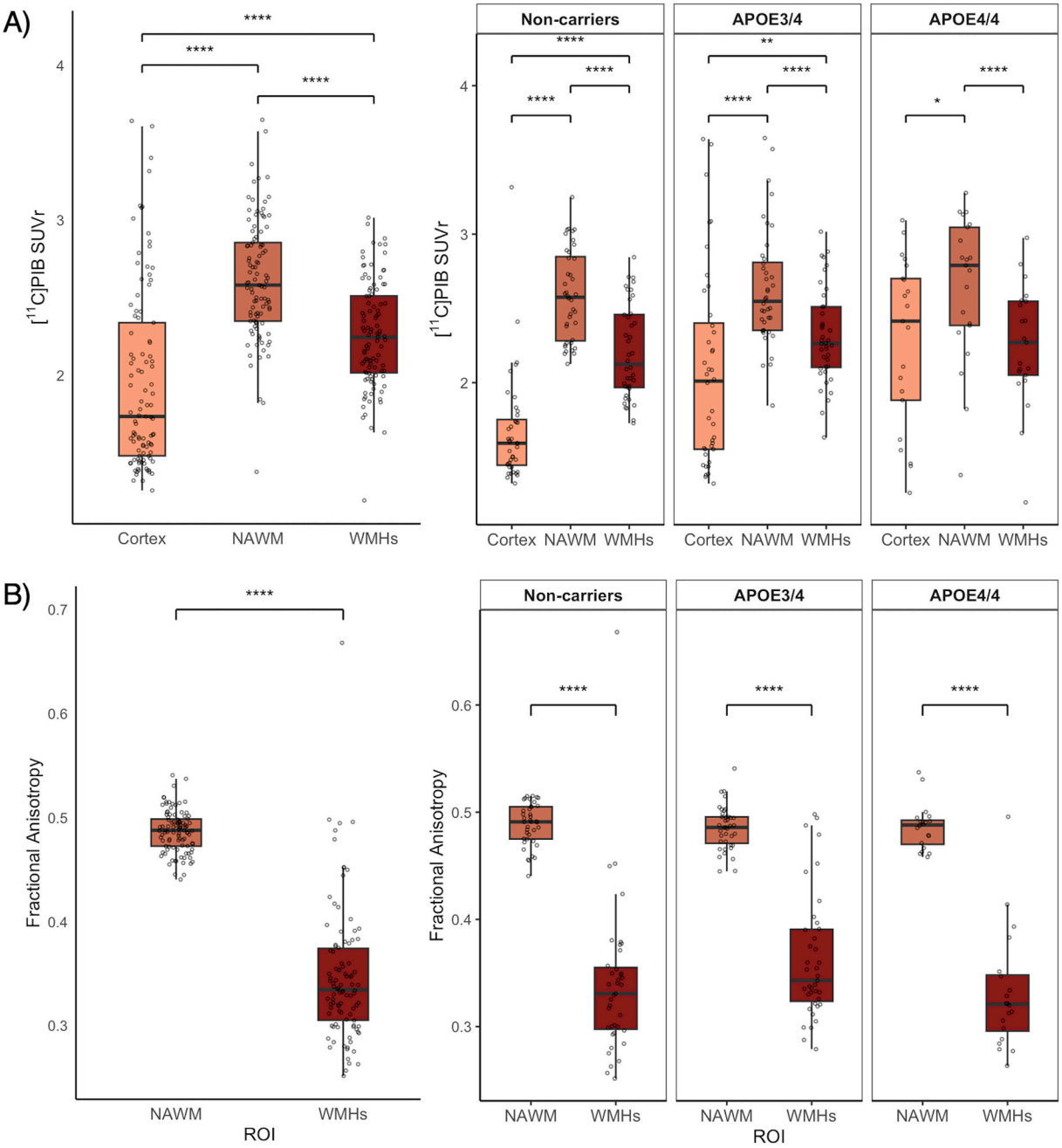

Fig. 3. [^{11}C]PiB SUVRs (3A) in cerebral cortex, NAWM and in WMHs and DTI-FA (3B) in NAWM and in WMHs in the total study population (left) and stratified by *APOE* genotype (right). Statistical significance is shown with star symbols (* p < 0.05, ** p < 0.01, *** p < 0.001, **** < 0.0001). NAWM = normal-appearing white matter, SUVR = standardized uptake value ratio, WMHs = white matter hyperintensities.

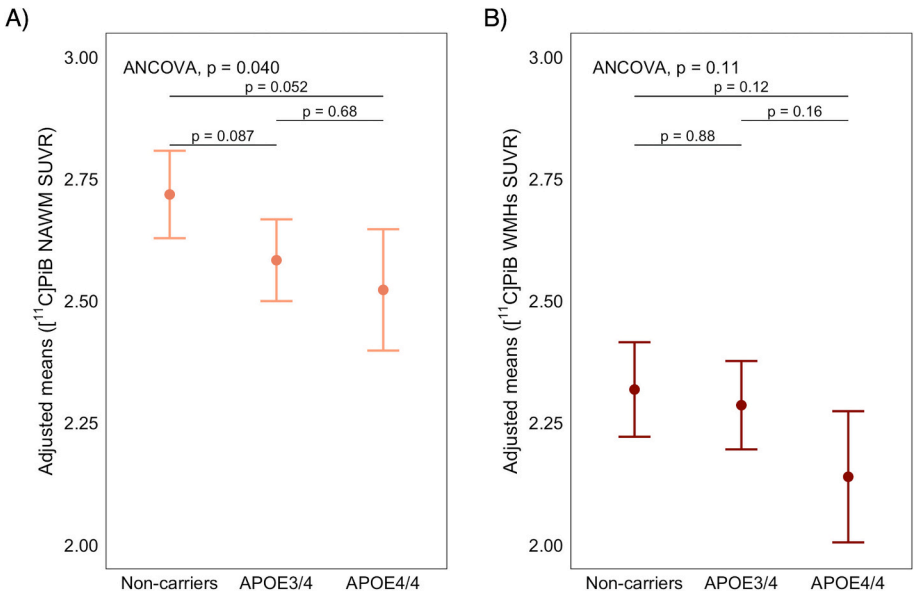

Fig. 4. Adjusted means from Type I ANCOVA (covariates were sex, age, global cortical [^{11}C]PiB SUVR and WMH volumes) within NAWM (4A) and WMHs (4B), showing average [^{11}C]PiB retention by *APOE* genotype (non-carriers, *APOE3/4* and *APOE4/4*) with confidence intervals at 95 % confidence level. NAWM = normal-appearing white matter, SUVRs = standardized uptake value ratios, WMHs = white matter hyperintensities.

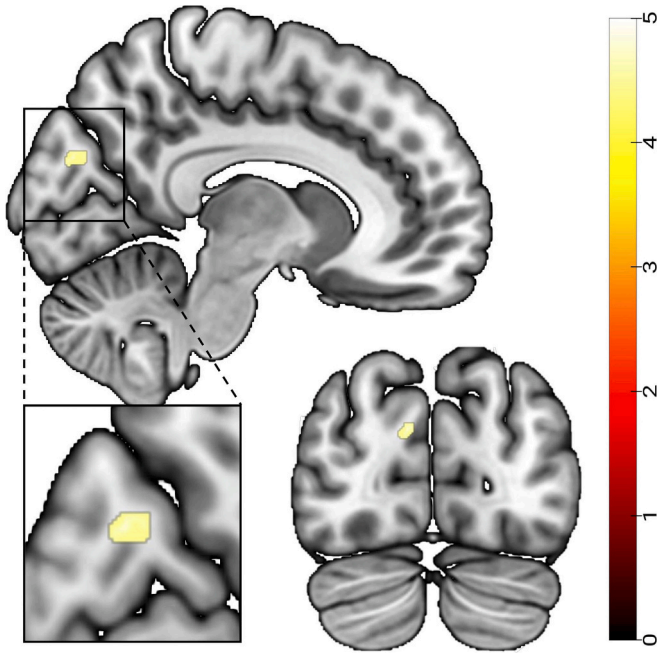

Fig. 5. Results from voxel-wise analysis comparing WM [^{11}C]PiB retention between non-carriers and *APOE4/4* carriers at $p_{FWE} < 0.05$ ($k \geq 83$), adjusted for sex, age, global cortical [^{11}C]PiB SUVR and WMH volumes.

where *APOE3/4* and *APOE4/4*, nor *APOE3/4* and non-carriers differed in WM [^{11}C]PiB retention at $p_{FWE} < 0.05$.

3.4. Relationship between DTI and WM [^{11}C]PiB PET

We did not find a correlation between DTI-FA and [^{11}C]PiB SUVRs in NAWM ($r_s = 0.075, p = 0.46$) whereas DTI-FA and [^{11}C]PiB SUVRs were weakly correlated in regions of WMHs ($r_s = 0.20$, $p = 0.048$). This relationship was further explored with a linear regression model, where WMHs [^{11}C]PiB SUVR was the dependent variable and WMHs DTI-FA was the independent variable, adjusted for age, sex, global cortical [^{11}C]PiB SUVR and WMH volumes. Within this model, the effect of DTI-FA on [^{11}C]PiB SUVRs was positive, but not statistically significant in regions of WMHs ($\beta = 0.54$, 95 % CI [−0.35, 1.43], $p = 0.23$, Fig. 6).

3.5. Sensitivity analysis

Differences in [^{11}C]PiB SUVR ($p_{paired\ t\text{-}test} < 0.001$) and DTI-FA ($p_{Wilcoxon} < 0.001$) between NAWM and regions of WMHs remained significant when individuals with low WMHs (< 1 cm^3) were removed from the analyses. In this subset of the population ($n = 82$), the three groups remained balanced in terms of age (F[2, 79] = 2.46, 95 % CI [0.00, 1.00], $p_{ANOVA} = 0.092$) and sex ($p_{Chi} = 0.55$), whereas they differed in global cortical [^{11}C]PiB SUVR ($p_{Kruskal\text{-}Wallis} < 0.001$). *APOE4/4* and *APOE3/4* carriers showed higher global cortical [^{11}C]PiB SUVRs than non-carriers ($p_{Dunn} < 0.001$ and $p_{Dunn} = 0.010$, respectively), as seen in the total study population. The effect of *APOE* on NAWM [^{11}C]PiB retention was statistically significant (F[2, 75] = 4.70,

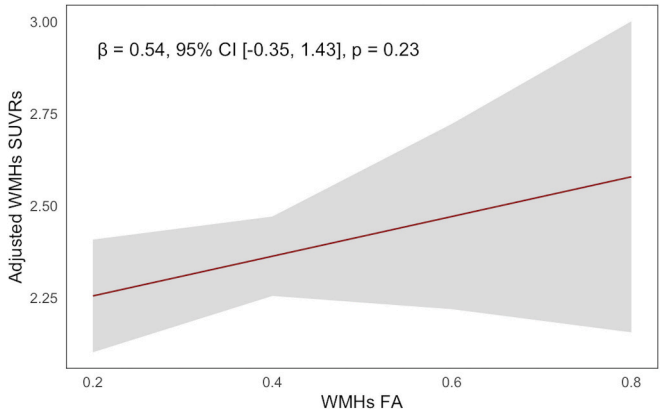

Fig. 6. Association between [^{11}C]PiB SUVRs and DTI-FA in regions of WMHs, adjusted for global cortical [^{11}C]PiB SUVR, age, sex and WMH volumes. X-axis showing the distribution of DTI-FA in regions of WMHs, Y-axis showing the predicted covariate-adjusted WMHs SUVRs from a linear regression model. The plot shows the regression line, and its confidence interval at 95 % confidence level. FA = Fractional anisotropy, SUVRs = Standardized uptake value ratios, WMHs = White matter hyperintensities.

95 % CI [0.02, 1.00], $p_{ANCOVA} = 0.012$, adjusted for global cortical [^{11}C]PiB SUVR, age, sex and WMH volumes), with *APOE4/4* carriers showing significantly lower NAWM SUVRs than non-carriers (95 % CI: [−0.45, −0.050], $p_{Tukey} = 0.011$). There were no significant differences between *APOE3/4* and *APOE4/4* carriers (95 % CI: [−0.28, 0.072], $p_{Tukey} = 0.33$), but there was a non-significant trend towards lower NAWM retention in *APOE3/4* compared to non-carriers (95 % CI: [−0.30, 0.0099], $p_{Tukey} = 0.071$). There were no significant differences in WMHs [^{11}C]PiB SUVRs in this subset ($F[2, 75] = 2.68$, 95 % CI [0.00, 1.00], $p_{ANCOVA} = 0.075$, adjusted for global cortical [^{11}C]PiB SUVR, age, sex and WMH volumes).

4. Discussion

Our findings indicate that the *APOE4* allele influences the binding of [^{11}C]PiB to myelin already in cognitively healthy older *APOE4* homozygotes. To our knowledge, this is the first study that investigated the separate effects of *APOE4* hetero- and homozygosity on WM [^{11}C]PiB PET retention in a cognitively healthy population. First, we found reductions in [^{11}C]PiB retention and DTI-FA within WMHs compared to NAWM in the total study population, in line with previous findings in the AD continuum (Moscoso et al., 2022; Rubinski et al., 2023). Second, in extension to earlier results, we stratified our cognitively healthy population into three groups based on their *APOE* genotype and found significant differences in NAWM [^{11}C]PiB SUVRs. *APOE4/4* carriers showed lower mean [^{11}C]PiB retention in NAWM, compared to non-carriers. However, this difference did not remain statistically significant in pairwise comparisons. Third, the regional analyses were further confirmed by additional voxel-wise analyses within cerebral WM, where *APOE4/4* carriers had lower WM [^{11}C]PiB retention than non-carriers in a small cluster adjacent to the right cuneus, whereas no other differences among the *APOE* genotypes were present at the specified threshold. Since AD progression inversely mirrors myelogenesis (Bartzokis et al., 2004), late-myelinating association fibers might be vulnerable at early stages of AD. A previous MRI study found demyelination in the cuneus among the best discriminating areas for late-onset AD (Fornari et al., 2012). Our results suggest that this pattern could appear unilaterally in cognitively healthy *APOE4/4* carriers, possibly progressing over the course of AD. However, since the pairwise comparisons were only borderline significant, claims of *APOE4*-related demyelination in this cohort should be made with caution. In line with previous studies (Fatemi et al., 2018), WMH load was higher in females. Sex alone did not have a significant effect on NAWM nor WMH [^{11}C]PiB SUVR ($p = 0.061$ and $p = 0.058$ respectively).

A voxel-wise reduction in [^{11}C]PiB retention has been reported in a previous study with patients with AD (de Faria et al., 2019), but the small sample size ($n = 36$) and lack of DTI data limited the interpretation of this finding. Moreover, the study did not explore whether retention decreases before diagnosis and did not explore tracer retention in NAWM and WMHs separately. Previous studies assessing [^{18}F]Florbetapir retention in WM were carried out with a larger number of participants (n = 115–795), including individuals with dementia (Moscoso et al., 2022; Ottoy et al., 2023; Rubinski et al., 2023); thus, we would expect possible demyelinating effects to be more subtle in a cognitively healthy population. Our sensitivity analysis evidenced that *APOE4/4* carriers with intermediate to high WMH volumes showed significantly lower [^{11}C]PiB NAWM SUVR than non-carriers. Therefore, it is unlikely that the decrease in myelin integrity found in the total sample of *APOE4/4* carriers reflected PVEs from these regions. On the contrary, it is possible that global WM demyelination is more extensive in individuals who have more WMHs, or that [^{11}C]PiB retention is decreased in NAWM surrounding regions of WMHs, as has been previously suggested (Carotenuto et al., 2020).

We did not find a correlation between NAWM [^{11}C]PiB SUVRs and NAWM DTI-FA in our study. Although we originally found a significant correlation between [^{11}C]PiB SUVRs and DTI-FA in regions of WMHs, the association was not significant in a linear model adjusted for the confounding effects. DTI-FA was chosen as an indicator of WM microstructure because it tends to correlate with histologically assessed myelin (Lazari and Lipp, 2021). However, the main contributor to anisotropy is the axonal membrane (van der Weijden et al., 2023), and DTI is sensitive to other WM microstructural properties than myelin, such as axonal degeneration. Therefore, lack of a correlation between DTI-FA and WM SUVRs does not challenge the validity of [^{11}C]PiB as a marker of myelin integrity. Because of the methodological differences between [^{11}C]PiB and DTI, these modalities might assess different tissue properties or WM fibers. DTI abnormalities in the context of AD are typically reported in deep WM tracts (Dowell et al., 2013; Gold et al., 2010; Tato-Fernández et al., 2024), whereas myelin-sensitive MRI such as magnetization transfer imaging found demyelinating patterns in superficial WM, including the cuneus (Fornari et al., 2012), an area where the *APOE4/4* carriers in our cohort showed lower [^{11}C]PiB retention. Lastly, these results could also be due to an insufficient sample size to reach the significance threshold, or the biological characteristics of our population. A correlation between WM retention of [^{18}F]Florbetapir and DTI-FA was previously reported (Moscoso et al., 2022; Ottoy et al., 2023), but the interpretation of this association is unclear. Previously, Moscoso et al. found an association between [^{18}F]Florbetapir NAWM SUVR and DTI-FA only within the AD continuum (Moscoso et al., 2022), meanwhile Ottoy et al. reported that [^{18}F]Florbetapir retention in regions of WMHs was more closely related to DTI-assessed free water than DTI-FA (Ottoy et al., 2023), which could indicate that the PET signal is linked with enlargement of the extracellular space rather than with WM microstructural properties. We did not correct DTI-FA for the contributions of free water, since our DTI acquisition protocol was not optimized for multi-compartmental models. It should be noted that both studies were carried out with [^{18}F]Florbetapir, and there may be additional differences in each tracer's affinity to myelin which have not yet been fully characterized.

Recently, *APOE4* homozygosity has been proposed as a genetic form of AD, which mirrors the biomarker changes found in autosomal AD (Fortea et al., 2024). WMHs are prominent in autosomal AD, even before the onset of dementia (Schoemaker et al., 2022). WM abnormalities could similarly be a feature of *APOE4* homozygosity. Cognitively healthy *APOE4* homozygotes in our sample showed reduced [^{11}C]PiB WM retention, indicating that [^{11}C]PiB-assessed WM impairment is associated with *APOE4* homozygosity early in the AD continuum and thus expanding the applications of this technique in the context of AD. The *APOE4* allele is strongly associated with Aβ aggregation (Cicognola et al., 2025; Fortea et al., 2024). Several factors involved in the production of Aβ have overlapping pathways with remyelination (Hirschfeld et al., 2022), and myelin pathology colocalizes with Aβ deposition in animal studies (Zhang et al., 2021b). It has been proposed that the pathological cascade seen in AD could be a result of insufficient myelin repair (Bartzokis, 2011; Depp et al., 2023). On the other hand, myelin impairment could be a byproduct of AD pathology, since Aβ is known to induce oligodendrocyte death, which again can hinder myelination (Blanchard et al., 2022; Lee et al., 2004). Moreover, impaired microglial function could explain the interaction between *APOE4* and myelin (Depp et al., 2023; Rubinski et al., 2023). If myelin impairment precedes the onset of clinical symptoms in *APOE4* carriers, targeting demyelination could be a promising avenue for future medications aimed at this group. Additional studies are required to understand the biological mechanisms underlying the role of demyelination in AD, and the validity of amyloid-PET for the measurement of myelin integrity.

The *APOE4/4* carriers of our cohort show abnormalities in imaging biomarkers, including structural and diffusion MRI and amyloid-PET (Koivumäki et al., 2024; Snellman et al., 2023; Tato-Fernández et al., 2024), but it is possible that demyelination precedes and is more closely related to cognitive deficits and tau pathology (Rubinski et al., 2023). NAWM [^{18}F]Florbetapir SUVR predicts longitudinal cognitive decline (Moscoso et al., 2022). Modulation of ApoE-related signaling pathways

might improve cognition and encourage remyelination (Hirschfeld et al., 2022). Put together, these findings suggest that WM [^{11}C]PiB retention could be a good biomarker to monitor disease progression and to assess the effects of remyelinating agents, but future longitudinal investigations are still necessary to further understand the interpretation of WM [^{11}C]PiB retention and its relationship with other biomarkers of AD.

One strength of this study is the possibility to compare the results of WM [^{11}C]PiB and DTI-FA in a cognitively normal sample with varying genetic risk for AD. We confirmed findings from previous studies on amyloid-PET to assess myelin in the context of AD with an independent cohort of cognitively unimpaired individuals, showing that these results are generalizable beyond the biological characteristics of a specific study population. [^{11}C]PiB was previously assessed as a marker of myelin integrity in multiple sclerosis and aging (Campanholo et al., 2022; Stankoff et al., 2011; Vavasour et al., 2022), and our study shows its applicability in the context of AD research. Moreover, we included a group of cognitively healthy *APOE4/4* carriers who are more than 65 years old, which allowed us to determine whether individuals at high genetic risk for AD show demyelination before disease onset.

This study has several limitations. While our cohort is relatively large for a multi-modal human neuroimaging study, our sample might be underpowered to detect subtle differences, given the smaller size of the *APOE4/4* carrier group ($n = 21$, *vs.* $n = 40$ in the other two groups), which may reduce the statistical power of *post-hoc* tests. Studying the effects of *APOE4* homozygosity in healthy elderly is challenging due to the low prevalence of this genotype and their high risk for sporadic AD. However, it has been reported that these individuals are more vulnerable to demyelination (Blanchard et al., 2022). Our main findings approached the significance threshold, and their robustness should be verified with independent cohorts. In order to assess the effects of *APOE4* carriership, our cohort is enriched with healthy older *APOE4* carriers, many of whom have Aβ in their brains. This resulted in uneven distributions of cortical [^{11}C]PiB SUVRs among the groups, which can confound the results. We took several steps to minimize PVEs, but WM and cortical SUVRs were still highly correlated. For that reason, all analyses were corrected for global cortical [^{11}C]PiB SUVR. This adjustment has a large impact on the comparisons, as shown in Tables A.1 and A.2, and causes discrepancy with studies whose populations had unknown or negative Aβ status. Lastly, [^{11}C]PiB SUVRs can be influenced by factors including blood flow, although a reduction of WM [^{11}C]PiB retention in *APOE4* homozygotes is unlikely due to WM kinetics alone (Kepe et al., 2013; Tohgi et al., 1998). Because of these shortcomings, we might not be able to estimate the full extent of demyelination using amyloid-PET. Further validation of WM amyloid-PET is still required to understand its relation to myelin integrity.

5. Conclusions

In conclusion, our results evidence a small decrease in WM [^{11}C]PiB retention already in cognitively unimpaired *APOE4* homozygotes. This finding suggests that *APOE4/4* carriers exhibit subtle demyelination before the onset of AD, but this effect is expected to become more apparent along with the development of cognitive symptoms. Larger studies including *APOE4/4* homozygotes should be carried out to confirm our results.

CRediT authorship contribution statement

Claudia Tato-Fernández: Writing – review & editing, Writing – original draft, Visualization, Formal analysis. **Laura L. Ekblad:** Writing – review & editing, Supervision, Project administration, Funding acquisition. **Marco Bucci:** Writing – review & editing, Validation, Resources. **Jouni Tuisku:** Writing – review & editing, Resources. **Riitta Parkkola:** Writing – review & editing, Methodology. **Semi Helin:** Writing – review & editing, Methodology. **Juha O. Rinne:** Writing – review & editing, Supervision, Funding acquisition, Conceptualization. **Anniina Snellman:** Writing – review & editing, Supervision, Project administration, Funding acquisition, Conceptualization.

Funding

CT received funding for this project from the Finnish Cultural Foundation, the Finnish Brain Foundation, Finnish Governmental Research Funding (VTR) and the University of Turku Graduate School. LLE was funded by the Finnish Medical Foundation, the Diabetes Research Foundation and by Finnish Governmental Research Funding (VTR) and she received project funding for the CIRI-5Y study from the Juho Vainio Foundation. JOR was funded by the Sigrid Juselius Foundation and Finnish Governmental Research Funding (VTR). AS was funded by the Research Council of Finland (grant number 341059), the Emil Aaltonen Foundation, the Paulo Foundation, Finnish Governmental Research Funding (VTR) and the Orion Research Foundation sr directly related to this study.

Declaration of competing interest

The authors declare that they have no known competing financial interests or personal relationships that could have appeared to influence the work reported in this paper.

Acknowledgements

The participants of ASIC-E4 and CIRI-5Y cohorts are warmly acknowledged for their commitment to the studies. The authors would additionally like to thank Alexis Moscoso Rial and Eliisa Löyttyniemi for their counseling on conducting the analyses.

Appendix A. Supplementary material

Shows results of sequential ANCOVA. Supplementary data to this article can be found online at [https://doi.org/10.1016/j.nbd.2025.107140].

Data availability

Data will be made available on reasonable request. Individual patient data cannot be made publicly available according to the institutional regulations and national legislation.

References

Bao, W., Jia, H., Finnema, S., Cai, Z., Carson, R.E., Huang, Y.H., 2017. PET imaging for early detection of Alzheimer's disease. PET Clin 12, 329–350. https://doi.org/10.1016/j.cpet.2017.03.001.

Bartzokis, G., 2011. Alzheimer's disease as homeostatic responses to age-related myelin breakdown. Neurobiol. Aging 32, 1341–1371. https://doi.org/10.1016/j.neurobiolaging.2009.08.007.

Bartzokis, G., Sultzer, D., Lu, P.H., Nuechterlein, K.H., Mintz, J., Cummings, J.L., 2004. Heterogeneous age-related breakdown of white matter structural integrity: implications for cortical "disconnection" in aging and Alzheimer's disease. Neurobiol. Aging 25, 843–851. https://doi.org/10.1016/j.neurobiolaging.2003.09.005.

Basser, P.J., Pierpaoli, C., 1996. Microstructural and physiological features of tissues elucidated by quantitative-diffusion-tensor MRI. J. Magn. Reson. B 111, 209–219. https://doi.org/10.1006/jmrb.1996.0086.

Blanchard, J.W., Akay, L.A., Davila-Velderrain, J., von Maydell, D., Mathys, H., Davidson, S.M., Effenberger, A., Chen, C.-Y., Maner-Smith, K., Hajjar, I., Ortlund, E. A., Bula, M., Agbas, E., Ng, A., Jiang, X., Kahn, M., Blanco-Duque, C., Lavoie, N., Liu, L., Reyes, R., Lin, Y.-T., Ko, T., R'Bibo, L., Ralvenius, W.T., Bennett, D.A., Cam, H.P., Kellis, M., Tsai, L.-H., 2022. APOE4 impairs myelination via cholesterol dysregulation in oligodendrocytes. Nature 611, 769–779. https://doi.org/10.1038/s41586-022-05439-w.

Bouhrara, M., Reiter, D.A., Bergeron, C.M., Zukley, L.M., Ferrucci, L., Resnick, S.M., Spencer, R.G., 2018. Evidence of demyelination in mild cognitive impairment and dementia using a direct and specific magnetic resonance imaging measure of myelin content. Alzheimers Dement. 14, 998–1004. https://doi.org/10.1016/j.jalz.2018.03.007.

Campanholo, K., Pitombeira, M., Rimkus, C., Mendes, M., Apóstolos-Pereira, S., Busatto Filho, G., Callegaro, D., Buchpiguel, C., Duran, F., De Paula Faria, D., 2022. Myelin imaging measures as predictors of cognitive impairment in MS patients: A hybrid PET-MRI study. Mult. Scler. Relat. Disord. 57, 103331. https://doi.org/10.1016/j.msard.2021.103331.

Carotenuto, A., Giordano, B., Dervenoulas, G., Wilson, H., Veronese, M., Chappell, Z., Polychronis, S., Pagano, G., Mackewn, J., Turkheimer, F.E., Williams, S.C.R., Hammers, A., Silber, E., Brex, P., Politis, M., 2020. [18F]Florbetapir PET/MR imaging to assess demyelination in multiple sclerosis. Eur. J. Nucl. Med. Mol. Imaging 47, 366–378. https://doi.org/10.1007/s00259-019-04533-y.

Chandler, M.J., Lacritz, L.H., Hynan, L.S., Barnard, H.D., Allen, G., Deschner, M., Weiner, M.F., Cullum, C.M., 2005. A total score for the CERAD neuropsychological battery. Neurology 65, 102–106. https://doi.org/10.1212/01.wnl.0000167607.63000.38.

Cicognola, C., Salvadó, G., Smith, R., Palmqvist, S., Stomrud, E., Betthauser, T., Johnson, S., Janelidze, S., Mattsson-Carlgren, N., Hansson, O., Pichet Binette, A., 2025. APOE4 impact on soluble and insoluble tau pathology is mostly influenced by amyloid-beta. Brain. https://doi.org/10.1093/brain/awaf016.

de Faria, D.P., Duran, F.L., Squarzoni, P., Coutinho, A.M., Garcez, A.T., Santos, P.P., Brucki, S.M., de Oliveira, M.O., Trés, E.S., Forlenza, O.V., Nitrini, R., Buchpiguel, C. A., Busatto Filho, G., 2019. Topography of 11C-Pittsburgh compound B uptake in Alzheimer's disease: a voxel-based investigation of cortical and white matter regions. Brazilian Journal of Psychiatry 41, 101–111. https://doi.org/10.1590/1516-4446-2017-0002.

Dean, D.C., Hurley, S.A., Kecskemeti, S.R., O'Grady, J.P., Canda, C., Davenport-Sis, N.J., Carlsson, C.M., Zetterberg, H., Blennow, K., Asthana, S., Sager, M.A., Johnson, S.C., Alexander, A.L., Bendlin, B.B., 2017. Association of amyloid pathology with myelin alteration in preclinical Alzheimer disease. JAMA Neurol. 74, 41–49. https://doi.org/10.1001/jamaneurol.2016.3232.

Depp, C., Sun, T., Sasmita, A.O., Spieth, L., Berghoff, S.A., Nazarenko, T., Overhoff, K., Steixner-Kumar, A.A., Subramanian, S., Arinrad, S., Ruhwedel, T., Möbius, W., Göbbels, S., Saher, G., Werner, H.B., Damkou, A., Zampar, S., Wirths, O., Thalmann, M., Simons, M., Saito, T., Saido, T., Krueger-Burg, D., Kawaguchi, R., Willem, M., Haass, C., Geschwind, D., Ehrenreich, H., Stassart, R., Nave, K.-A., 2023. Myelin dysfunction drives amyloid-β deposition in models of Alzheimer's disease. Nature. https://doi.org/10.1038/s41586-023-06120-6.

Dowell, N.G., Ruest, T., Evans, S.L., King, S.L., Tabet, N., Tofts, P.S., Rusted, J.M., 2013. MRI of carriers of the apolipoprotein E e4 allele-evidence for structural differences in normal-appearing brain tissue in e4+ relative to e4- young adults. NMR Biomed. 26, 674–682. https://doi.org/10.1002/nbm.2912.

Ekblad, L.L., Johansson, J., Helin, S., Viitanen, M., Laine, H., Puukka, P., Jula, A., Rinne, J.O., 2018. Midlife insulin resistance, APOE genotype, and late-life brain amyloid accumulation. Neurology 90, 1150–1157. https://doi.org/10.1212/WNL.0000000000005214.

Fatemi, F., Kantarci, K., Graff-Radford, J., Preboske, G.M., Weigand, S.D., Przybelski, S. A., Knopman, D.S., Machulda, M.M., Roberts, R.O., Mielke, M.M., Petersen, R.C., Jack, C.R., Vemuri, P., 2018. Sex differences in cerebrovascular pathologies on FLAIR in cognitively unimpaired elderly. Neurology 90. https://doi.org/10.1212/WNL.0000000000004913.

Fodero-Tavoletti, M.T., Rowe, C.C., McLean, C.A., Leone, L., Li, Q.-X., Masters, C.L., Cappai, R., Villemagne, V.L., 2009. Characterization of PiB binding to White matter in Alzheimer disease and other dementias. J. Nucl. Med. 50, 198–204. https://doi.org/10.2967/jnumed.108.057984.

Fornari, E., Maeder, P., Meuli, R., Ghika, J., Knyazeva, M.G., 2012. Demyelination of superficial white matter in early Alzheimer's disease: a magnetization transfer imaging study. Neurobiol. Aging 33, 428.e7–428.e19. https://doi.org/10.1016/j.neurobiolaging.2010.11.014.

Fortea, J., Pegueroles, J., Alcolea, D., Belbin, O., Dols-Icardo, O., Vaqué-Alcázar, L., Videla, L., Gispert, J.D., Suárez-Calvet, M., Johnson, S.C., Sperling, R., Bejanin, A., Lleó, A., Montal, V., 2024. APOE4 homozygosity represents a distinct genetic form of Alzheimer's disease. Nat. Med. 30, 1284–1291. https://doi.org/10.1038/s41591-024-02931-w.

Fox, J., 2008. Applied Regression Analysis and Generalized Linear Models, 2nd, Edition. ed. Sage, Los Angeles.

Gold, B.T., Powell, D.K., Andersen, A.H., Smith, C.D., 2010. Alterations in multiple measures of white matter integrity in normal women at high risk for Alzheimer's disease. Neuroimage 52, 1487–1494. https://doi.org/10.1016/j.neuroimage.2010.05.036.

Grothe, M.J., Barthel, H., Sepulcre, J., Dyrba, M., Sabri, O., Teipel, S.J., Weiner, Michael, Aisen, P., Weiner, Michael, Aisen, P., Petersen, R., Jack, C.R., Jagust, W., Trojanowki, John Q., Toga, A.W., Beckett, L., Green, R.C., Saykin, A.J., Morris, J., Liu, E., Green, R.C., Montine, T., Petersen, R., Aisen, P., Gamst, A., Thomas, R.G., Donohue, M., Walter, S., Gessert, D., Sather, T., Beckett, L., Harvey, D., Gamst, A., Donohue, M., Kornak, J., Jack, C.R., Dale, A., Bernstein, M., Felmlee, J., Fox, N., Thompson, P., Schuff, N., Alexander, G., DeCarli, C., Jagust, W., Bandy, D., Koeppe, R.A., Foster, N., Reiman, E.M., Chen, K., Mathis, C., Morris, J., Cairns, N.J., Taylor-Reinwald, L., Trojanowki, J.Q., Shaw, L., Lee, V.M.Y., Korecka, M., Toga, A. W., Crawford, K., Neu, S., Saykin, A.J., Foroud, T.M., Potkin, S., Shen, L., Kachaturian, Z., Frank, R., Snyder, P.J., Molchan, S., Kaye, J., Quinn, J., Lind, B., Dolen, S., Schneider, L.S., Pawluczyk, S., Spann, B.M., Brewer, J., Vanderswag, H., Heidebrink, J.L., Lord, J.L., Petersen, R., Johnson, Kris, Doody, R.S., Villanueva-Meyer, J., Chowdhury, M., Stern, Y., Honig, L.S., Bell, K.L., Morris, J.C., Ances, B., Carroll, M., Leon, S., Mintun, M.A., Schneider, S., Marson, D., Griffith, R., Clark, D., Grossman, H., Mitsis, E., Romirowsky, A., deToledo-Morrell, L., Shah, R.C., Duara, R., Varon, D., Roberts, P., Albert, M., Onyike, C., Kielb, S., Rusinek, H., de Leon, M.J., Glodzik, L., De Santi, S., Doraiswamy, P.M., Petrella, J.R., Coleman, R.E., Arnold, S.E., Karlawish, J.H., Wolk, D., Smith, C.D., Jicha, G., Hardy, P., Lopez, O.L., Oakley, M., Simpson, D.M., Porsteinsson, A.P., Goldstein, B.S., Martin, K., Makino, K. M., Ismail, M.S., Brand, C., Mulnard, R.A., Thai, G., Mc-Adams-Ortiz, C., Womack, K., Mathews, D., Quiceno, M., Diaz-Arrastia, R., King, R., Weiner, Myron, Martin-Cook, K., DeVous, M., Levey, A.I., Lah, J.J., Cellar, J.S., Burns, J.M., Anderson, H.S., Swerdlow, R.H., Apostolova, L., Lu, P.H., Bartzokis, G., Silverman, D.H.S., Parfitt, F., Johnson, H., Farlow, M.R., Hake, A.M., Matthews, B.R., Herring, S., van Dyck, C.H., Carson, R.E., MacAvoy, M.G., Chertkow, H., Bergman, H., Hosein, C., Black, S., Stefanovic, B., Caldwell, C., Robin Hsiung, G.-Y., Feldman, H., Mudge, B., Assaly, M., Kertesz, A., Rogers, J., Trost, D., Bernick, C., Munic, D., Kerwin, D., Mesulam, M.-M., Lipowski, K., Wu, C.-K., Johnson, N., Sadowsky, C., Martinez, W., Villena, T., Turner, R.S., Johnson, Kathleen, Reynolds, B., Sperling, R.A., Johnson, K.A., Marshall, G., Frey, M., Yesavage, J., Taylor, J.L., Lane, B., Rosen, A., Tinklenberg, J., Sabbagh, M., Belden, C., Jacobson, S., Kowall, N., Killiany, R., Budson, A.E., Norbash, A., Johnson, P.L., Obisesan, T.O., Wolday, S., Bwayo, S.K., Lerner, A., Hudson, L., Ogrocki, P., Fletcher, E., Carmichael, O., Olichney, J., DeCarli, C., Kittur, S., Borrie, M., Lee, T.-Y., Bartha, R., Johnson, S., Asthana, S., Carlsson, C.M., Potkin, S.G., Preda, A., Nguyen, D., Tariot, P., Fleisher, A., Reeder, S., Bates, V., Capote, H., Rainka, M., Scharre, D.W., Kataki, M., Zimmerman, E.A., Celmins, D., Brown, A.D., Pearlson, G. D., Blank, K., Anderson, K., Saykin, A.J., Santulli, R.B., Schwartz, E.S., Sink, K.M., Williamson, J.D., Garg, P., Watkins, F., Ott, B.R., Querfurth, H., Tremont, G., Salloway, S., Malloy, P., Correia, S., Rosen, H.J., Miller, B.L., Mintzer, J., Longmire, C.F., Spicer, K., Finger, E., Rachinsky, I., Rogers, J., Kertesz, A., Drost, D., Pomara, N., Hernando, R., Sarrael, A., Schultz, S.K., Boles Ponto, L.L., Shim, H., Smith, K.E., Relkin, N., Chaing, G., Raudin, L., Smith, A., Fargher, K., Raj, B.A., 2017. In vivo staging of regional amyloid deposition. Neurology 89, 2031–2038. https://doi.org/10.1212/WNL.0000000000004643.

Hirschfeld, L.R., Risacher, S.L., Nho, K., Saykin, A.J., 2022. Myelin repair in Alzheimer's disease: a review of biological pathways and potential therapeutics. Transl Neurodegener 11, 47. https://doi.org/10.1186/s40035-022-00321-1.

Karjalainen, T., Tuisku, J., Santavirta, S., Kantonen, T., Bucci, M., Tuominen, L., Hirvonen, J., Hietala, J., Rinne, J.O., Nummenmaa, L., 2020. Magia: robust automated image processing and kinetic Modeling toolbox for PET Neuroinformatics. Front. Neuroinform. 14. https://doi.org/10.3389/fninf.2020.00003.

Kepe, V., Moghbel, M.C., Långström, B., Zaidi, H., Vinters, H.V., Huang, S.-C., Satyamurthy, N., Doudet, D., Mishani, E., Cohen, R.M., Høilund-Carlsen, P.F., Alavi, A., Barrio, J.R., 2013. Amyloid-β positron emission tomography imaging probes: A critical review. J Alzheimer's Dis 36, 613–631. https://doi.org/10.3233/JAD-130485.

Klunk, W.E., Engler, H., Nordberg, A., Wang, Y., Blomqvist, G., Holt, D.P., Bergström, M., Savitcheva, I., Huang, G., Estrada, S., Ausén, B., Debnath, M.L., Barletta, J., Price, J. C., Sandell, J., Lopresti, B.J., Wall, A., Koivisto, P., Antoni, G., Mathis, C.A., Långström, B., 2004. Imaging brain amyloid in Alzheimer's disease with Pittsburgh compound-B. Ann. Neurol. 55, 306–319. https://doi.org/10.1002/ana.20009.

Koikkalainen, J., Rhodius-Meester, H., Tolonen, A., Barkhof, F., Tijms, B., Lemstra, A.W., Tong, T., Guerrero, R., Schuh, A., Ledig, C., Rueckert, D., Soininen, H., Remes, A.M., Waldemar, G., Hasselbalch, S., Mecocci, P., Van Der Flier, W., Lötjönen, J., 2016. Differential diagnosis of neurodegenerative diseases using structural MRI data. Neuroimage Clin 11, 435–449. https://doi.org/10.1016/j.nicl.2016.02.019.

Koivumäki, M., Ekblad, L., Lantero-Rodriguez, J., Ashton, N.J., Karikari, T.K., Helin, S., Parkkola, R., Lötjönen, J., Zetterberg, H., Blennow, K., Rinne, J.O., Snellman, A., 2024. Blood biomarkers of neurodegeneration associate differently with amyloid deposition, medial temporal atrophy, and cerebrovascular changes in APOE ε4-enriched cognitively unimpaired elderly. Alzheimer's Res Ther 16, 112. https://doi.org/10.1186/s13195-024-01477-w.

Landau, S.M., Thomas, B.A., Thurfjell, L., Schmidt, M., Margolin, R., Mintun, M., Pontecorvo, M., Baker, S.L., Jagust, W.J., 2014. Amyloid PET imaging in Alzheimer's disease: a comparison of three radiotracers. Eur. J. Nucl. Med. Mol. Imaging 41, 1398–1407. https://doi.org/10.1007/s00259-014-2753-3.

Lazari, A., Lipp, I., 2021. Can MRI measure myelin? Systematic review, qualitative assessment, and meta-analysis of studies validating microstructural imaging with myelin histology. Neuroimage 230, 117744. https://doi.org/10.1016/j.neuroimage.2021.117744.

Lee, J.-T., Xu, J., Lee, J.-M., Ku, G., Han, X., Yang, D.-I., Chen, S., Hsu, C.Y., 2004. Amyloid-β peptide induces oligodendrocyte death by activating the neutral sphingomyelinase–ceramide pathway. J. Cell Biol. 164, 123–131. https://doi.org/10.1083/jcb.200307017.

Lopresti, B.J., Klunk, W.E., Mathis, C.A., Hoge, J.A., Ziolko, S.K., Lu, X., Meltzer, C.C., Schimmel, K., Tsopelas, N.D., DeKosky, S.T., Price, J.C., 2005. Simplified quantification of Pittsburgh compound B amyloid imaging PET studies: a comparative analysis. J. Nucl. Med. 46, 1959–1972.

Moscoso, A., Silva-Rodríguez, J., Aldrey, J.M., Cortés, J., Pías-Peleteiro, J.M., Ruibal, Á., Aguiar, P., 2022. 18F-florbetapir PET as a marker of myelin integrity across the Alzheimer's disease spectrum. Eur. J. Nucl. Med. Mol. Imaging 49, 1242–1253. https://doi.org/10.1007/s00259-021-05493-y.

Nichols, E., Steinmetz, J.D., Vollset, S.E., Fukutaki, K., Chalek, J., Abd-Allah, F., Abdoli, A., Abualhasan, A., Abu-Gharbieh, E., Akram, T.T., Al Hamad, H., Alahdab, F., Alanezi, F.M., Alipour, V., Almustanyir, S., Amu, H., Ansari, I., Arabloo, J., Ashraf, T., Astell-Burt, T., Ayano, G., Ayuso-Mateos, J.L., Baig, A.A., Barnett, A., Barrow, A., Baune, B.T., Béjot, Y., Bezabhe, W.M.M., Bezabih, Y.M., Bhagavathula, A.S., Bhaskar, S., Bhattacharyya, K., Bijani, A., Biswas, A., Bolla, S.R., Boloor, A., Brayne, C., Brenner, H., Burkart, K., Burns, R.A., Cámera, L.A., Cao, C., Carvalho, F., Castro-de-Araujo, L.F.S., Catalá-López, F., Cerin, E., Chavan, P.P., Cherbuin, N., Chu, D.-T., Costa, V.M., Couto, R.A.S., Dadras, O., Dai, X., Dandona, L.,

Dandona, R., De la Cruz-Góngora, V., Dhamnetiya, D., Dias da Silva, D., Diaz, D., Douiri, A., Edvardsson, D., Ekholuenetale, M., El Sayed, I., El-Jaafary, S.I., Eskandari, K., Eskandarieh, S., Esmaeilnejad, S., Fares, J., Faro, A., Farooque, U., Feigin, V.L., Feng, X., Fereshtehnejad, S.-M., Fernandes, E., Ferrara, P., Filip, I., Fillit, H., Fischer, F., Gaidhane, S., Galluzzo, L., Ghashghaee, A., Ghith, N., Gialluisi, A., Gilani, S.A., Glavan, I.-R., Gnedovskaya, E.V., Golechha, M., Gupta, R., Gupta, V.B., Gupta, V.K., Haider, M.R., Hall, B.J., Hamidi, S., Hanif, A., Hankey, G.J., Haque, S., Hartono, R.K., Hasaballah, A.I., Hasan, M.T., Hassan, A., Hay, S.I., Hayat, K., Hegazy, M.I., Heidari, G., Heidari-Soureshjani, R., Herteliu, C., Househ, M., Hussain, R., Hwang, B.-F., Iacoviello, L., Iavicoli, I., Ilesanmi, O.S., Ilic, I.M., Ilic, M.D., Irvani, S.S.N., Iso, H., Iwagami, M., Jabbarinejad, R., Jacob, L., Jain, V., Jayapal, S.K., Jayawardena, R., Jha, R.P., Jonas, J.B., Joseph, N., Kalani, R., Kandel, A., Kandel, H., Karch, A., Kasa, A.S., Kassie, G.M., Keshavarz, P., Khan, M.A., Khatib, M.N., Khoja, T.A.M., Khubchandani, J., Kim, M.S., Kim, Y.J., Kisa, A., Kisa, S., Kivimäki, M., Koroshetz, W.J., Koyanagi, A., Kumar, G.A., Kumar, M., Lak, H.M., Leonardi, M., Li, B., Lim, S.S., Liu, X., Liu, Y., Logroscino, G., Lorkowski, S., Lucchetti, G., Lutzky Saute, R., Magnani, F.G., Malik, A.A., Massano, J., Mehndiratta, M.M., Menezes, R.G., Meretoja, A., Mohajer, B., Mohamed Ibrahim, N., Mohammad, Y., Mohammed, A., Mokdad, A.H., Mondello, S., Moni, M. A.A., Moniruzzaman, M., Mossie, T.B., Nagel, G., Naveed, M., Nayak, V.C., Neupane Kandel, S., Nguyen, T.H., Oancea, B., Otstavnov, N., Otstavnov, S.S., Owolabi, M.O., Panda-Jonas, S., Pashazadeh Kan, F., Pasovic, M., Patel, U.K., Pathak, M., Peres, M.F. P., Perianayagam, A., Peterson, C.B., Phillips, M.R., Pinheiro, M., Piradov, M.A., Pond, C.D., Potashman, M.H., Pottoo, F.H., Prada, S.I., Radfar, A., Raggi, A., Rahim, F., Rahman, M., Ram, P., Ranasinghe, P., Rawaf, D.L., Rawaf, S., Rezaei, N., Rezapour, A., Robinson, S.R., Romoli, M., Roshandel, G., Sahathevan, R., Sahebkar, A., Sahraian, M.A., Sathian, B., Sattin, D., Sawhney, M., Saylan, M., Schiavolin, S., Seylani, A., Sha, F., Shaikh, M.A., Shaji, K., Shannawaz, M., Shetty, J. K., Shigematsu, M., Shin, J. Il, Shiri, R., Silva, D.A.S., Silva, J.P., Silva, R., Singh, J. A., Skryabin, V.Y., Skryabina, A.A., Smith, A.E., Soshnikov, S., Spurlock, E.E., Stein, D.J., Sun, J., Tabarés-Seisdedos, R., Thakur, B., Timalsina, B., Tovani-Palone, M.R., Tran, B.X., Tsegaye, G.W., Valadan Tahbaz, S., Valdez, P.R., Venketasubramanian, N., Vlassov, V., Vu, G.T., Vu, L.G., Wang, Y.-P., Wimo, A., Winkler, A.S., Yadav, L., Yahyazadeh Jabbari, S.H., Yamagishi, K., Yang, L., Yano, Y., Yonemoto, N., Yu, C., Yunusa, I., Zadey, S., Zastrozhin, M.S., Zastrozhina, A., Zhang, Z.-J., Murray, C.J.L., Vos, T., 2022. Estimation of the global prevalence of dementia in 2019 and forecasted prevalence in 2050: an analysis for the global burden of disease study 2019. Lancet Public Health 7, e105–e125. https://doi.org/10.1016/S2468-2667(21)00249-8.

Ottoy, J., Ozzoude, M., Zukotynski, K., Kang, M.S., Adamo, S., Scott, C., Ramirez, J., Swardfager, W., Lam, B., Bhan, A., Mojiri, P., Kiss, A., Strother, S., Bocti, C., Borrie, M., Chertkow, H., Frayne, R., Hsiung, R., Laforce, R.J., Noseworthy, M.D., Prato, F.S., Sahlas, D.J., Smith, E.E., Kuo, P.H., Chad, J.A., Pasternak, O., Sossi, V., Thiel, A., Soucy, J.P., Tardif, J.C., Black, S.E., Goubran, M., 2023. Amyloid-PET of the white matter: relationship to free water, fiber integrity, and cognition in patients with dementia and small vessel disease. J. Cereb. Blood Flow Metab. https://doi.org/10.1177/0271678X231152001.

Pietilä, E., Snellman, A., Tuisku, J., Helin, S., Viitanen, M., Jula, A., Rinne, J.O., Ekblad, L.L., 2024. Midlife insulin resistance, APOE genotype, and change in late-life brain beta-amyloid accumulation – A 5-year follow-up [11C]PIB-PET study. Neurobiol. Dis. 190, 106385. https://doi.org/10.1016/j.nbd.2023.106385.

Pietroboni, A.M., Colombi, A., Carandini, T., Sacchi, L., Fenoglio, C., Marotta, G., Arighi, A., De Riz, M.A., Fumagalli, G.G., Castellani, M., Bozzali, M., Scarpini, E., Galimberti, D., 2022. Amyloid PET imaging and dementias: potential applications in detecting and quantifying early white matter damage. Alzheimer's Res Ther 14. https://doi.org/10.1186/s13195-021-00933-1.

Rubinski, A., Dewenter, A., Zheng, L., Franzmeier, N., Stephenson, H., Deming, Y., Duering, M., Gesierich, B., Denecke, J., Pham, A.V., Bendlin, B., Ewers, M., 2023. Florbetapir PET-assessed demyelination is associated with faster tau accumulation in an APOE ε4-dependent manner. Eur. J. Nucl. Med. Mol. Imaging. https://doi.org/10.1007/s00259-023-06530-8.

Schoemaker, D., Zanon Zotin, M.C., Chen, K., Igwe, K.C., Vila-Castelar, C., Martinez, J., Baena, A., Fox-Fuller, J.T., Lopera, F., Reiman, E.M., Brickman, A.M., Quiroz, Y.T., 2022. White matter hyperintensities are a prominent feature of autosomal dominant Alzheimer's disease that emerge prior to dementia. Alzheimer's Res Ther 14, 89. https://doi.org/10.1186/s13195-022-01030-7.

Shirzadi, Z., Schultz, S.A., Yau, W.-Y.W., Joseph-Mathurin, N., Fitzpatrick, C.D., Levin, R., Kantarci, K., Preboske, G.M., Jack, C.R., Farlow, M.R., Hassenstab, J., Jucker, M., Morris, J.C., Xiong, C., Karch, C.M., Levey, A.I., Gordon, B.A., Schofield, P.R., Salloway, S.P., Perrin, R.J., McDade, E., Levin, J., Cruchaga, C., Allegri, R.F., Fox, N.C., Goate, A., Day, G.S., Koeppe, R., Chui, H.C., Berman, S., Mori, H., Sanchez-Valle, R., Lee, J.-H., Rosa-Neto, P., Ruthirakuhan, M., Wu, C.-Y., Swardfager, W., Benzinger, T.L.S., Sohrabi, H.R., Martins, R.N., Bateman, R.J., Johnson, K.A., Sperling, R.A., Greenberg, S.M., Schultz, A.P., Chhatwal, J.P., Weiner, M.W., Aisen, P., Petersen, R., Jack, C.R., Jagust, W., Trojanowki, J.Q., Toga, A.W., Beckett, L., Green, R.C., Saykin, A.J., Morris, J.C., Perrin, R.J., Shaw, L. M., Khachaturian, Z., Carrillo, M., Potter, W., Barnes, L., Bernard, M., González, H., Ho, C., Hsiao, J.K., Jackson, J., Masliah, E., Masterman, D., Okonkwo, O., Ryan, L., Silverberg, N., Fleisher, A., Sacrey, D.T., Fockler, J., Conti, C., Veitch, D., Neuhaus, J., Jin, C., Nosheny, R., Ashford, M., Flenniken, D., Kormos, A., Montine, T., Rafii, M., Raman, R., Jimenez, G., Donohue, M., Gessert, D., Salazar, J., Zimmerman, C., Cabrera, Y., Walter, S., Miller, G., Coker, G., Clanton, T., Hergesheimer, L., Smith, S., Adegoke, O., Mahboubi, P., Moore, S., Pizzola, J., Shaffer, E., Sloan, B., Harvey, D., Forghanian-Arani, A., Borowski, B., Ward, C., Schwarz, C., Jones, D., Gunter, J., Kantarci, K., Senjem, M., Vemuri, P., Reid, R., Fox, N.C., Malone, I., Thompson, P., Thomopoulos, S.I., Nir, T.M., Jahanshad, N., DeCarli, C., Knaack, A., Fletcher, E., Tosun-Turgut, D., Chen, S.R., Choe, M., Crawford, K., Yushkevich, P.A., Das, S., Koeppe, R.A., Reiman, E.M., Chen, K., Mathis, C., Landau, S., Cairns, N.J., Householder, E., Franklin, E., Bernhardt, H., Taylor-Reinwald, L., Korecka, M., Figurski, M., Neu, S., Nho, K., Risacher, S.L., Apostolova, L.G., Shen, L., Foroud, T.M., Nudelman, K., Faber, K., Wilmes, K., Thal, L., Silbert, L.C., Lind, B., Crissey, R., Kaye, J.A., Carter, R., Dolen, S., Quinn, J., Schneider, L.S., Pawluczyk, S., Becerra, M., Teodoro, L., Dagerman, K., Spann, B.M., Brewer, J., Vanderswag, H., Ziolkowski, J., Heidebrink, J.L., Zbizek-Nulph, L., Lord, J.L., Mason, S.S., Albers, C.S., Knopman, D., Johnson, Kris, Villaneuva-Meyer, J., Pavlik, V., Pacini, N., Lamb, A., Kass, J.S., Doody, R.S., Shibley, V., Chowdhury, M., Rountree, S., Dang, M., Stern, Y., Honig, L.S., Mintz, A., Ances, B., Winkfield, D., Carroll, M., Stobbs-Cucchi, G., Oliver, A., Creech, M.L., Mintun, M.A., Schneider, S., Geldmacher, D., Love, M.N., Griffith, R., Clark, D., Brockington, J., Marson, D., Grossman, H., Goldstein, M.A., Greenberg, J., Mitsis, E., Shah, R.C., Lamar, M., Samuels, P., Duara, R., Greig-Custo, M.T., Rodriguez, R., Albert, M., Onyike, C., Farrington, L., Rudow, S., Brichko, R., Kielb, S., Smith, A., Raj, B.A., Fargher, K., Sadowski, M., Wisniewski, T., Shulman, M., Faustin, A., Rao, J., Castro, K.M., Ulysse, A., Chen, S., Sheikh, M.O., Singleton-Garvin, J., Doraiswamy, P. M., Petrella, J.R., James, O., Wong, T.Z., Borges-Neto, S., Karlawish, J.H., Wolk, D. A., Vaishnavi, S., Clark, C.M., Arnold, S.E., Smith, C.D., Jicha, G.A., El Khouli, R., Raslau, F.D., Lopez, O.L., Oakley, M., Simpson, D.M., Porsteinsson, A.P., Martin, K., Kowalski, N., Keltz, M., Goldstein, B.S., Makino, K.M., Ismail, M.S., Brand, C., Thai, G., Pierce, A., Yanez, B., Sosa, E., Witbracht, M., Kelley, B., Nguyen, T., Womack, K., Mathews, D., Quiceno, M., Levey, A.I., Lah, J.J., Hajjar, I., Cellar, J.S., Burns, J.M., Swerdlow, R.H., Brooks, W.M., Silverman, D.H.S., Kremen, S., Tingus, K., Lu, P.H., Bartzokis, G., Woo, E., Teng, E., Graff-Radford, N.R., Parfitt, F., Poki-Walker, K., Farlow, M.R., Hake, A.M., Matthews, B.R., Brosch, J.R., Herring, S., van Dyck, C.H., Mecca, A.P., Good, S.P., MacAvoy, M.G., Carson, R.E., Varma, P., Chertkow, H., Vaitekunis, S., Hosein, C., Black, S., Stefanovic, B., Heyn, C. Chinthaka, Hsiung, G.-Y.R., Kim, E., Mudge, B., Sossi, V., Feldman, H., Assaly, M., Finger, E., Pasternak, S., Rachinsky, I., Kertesz, A., Drost, D., Rogers, J., Grant, I., Muse, B., Rogalski, E., Robson, J., Mesulam, M.-M., Kerwin, D., Wu, C.-K., Johnson, N., Lipowski, K., Weintraub, S., Bonakdarpour, B., Pomara, N., Hernando, R., Sarrael, A., Rosen, H.J., Miller, B.L., Perry, D., Turner, R.S., Johnson, Kathleen, Reynolds, B., MCCann, K., Poe, J., Sperling, R.A., Johnson, K.A., Marshall, G.A., Yesavage, J., Taylor, J.L., Chao, S., Coleman, J., White, J.D., Lane, B., Rosen, A., Tinklenberg, J., Belden, C.M., Atri, A., Clark, K.A., Zamrini, E., Sabbagh, M., Killiany, R., Stern, R., Mez, J., Kowall, N., Budson, A.E., Obisesan, T.O., Ntekim, O.E., Wolday, S., Khan, J.I., Nwulia, E., Nadarajah, S., Lerner, A., Ogrocki, P., Tatsuoka, C., Fatica, P., Maillard, P., Olichney, J., Carmichael, O., Bates, V., Capote, H., Rainka, M., Borrie, M., Lee, T.-Y., Bartha, R., Johnson, S., Asthana, S., Carlsson, C.M., Perrin, A., Burke, A., Scharre, D.W., Kataki, M., Tarawneh, R., Hart, D., Zimmerman, E.A., Celmins, D., Miller, D.D., Boles Ponto, L. L., Smith, K.E., Koleva, H., Shim, H., Nam, K.W., Schtulz, S.K., Williamson, J.D., Craft, S., Cleveland, J., Yang, M., Sink, K.M., Ott, B.R., Drake, J., Tremont, G., Daiello, L.A., Ritter, A., Bernick, C., Munic, D., O'Connell, A., Mintzer, J., Wiliams, A., Masdeu, J., Shi, J., Garcia, A., Newhouse, P., Potkin, S., Salloway, S., Malloy, P., Correia, S., Kittur, S., Pearlson, G.D., Blank, K., Anderson, K., Flashman, L.A., Seltzer, M., Hynes, M.L., Santulli, R.B., Relkin, N., Chiang, G., Lee, A., Lin, M., Ravdin, L., Sood, A., Blanchard, K.S., Fleischman, D., Arfanakis, K., Varon, D., Greig, M.T., Goldstein, B., Martin, K.S., Reist, C., Sadowsky, C., Martinez, W., Villena, T., Rosen, H., Marshall, G., Peskind, E.R., Petrie, E.C., Li, G., Noble, J.M., Voglein, J., Chrem Mendez, P., Surace, E., Ikonomovic, S., Nadkarni, N. K., Lopera, F., Ramirez, L., Aguillon, D., Leon, Y., Ramos, C., Alzate, D., Baena, A., Londono, N., Moreno, S., Laske, C., Kuder-Buletta, E., Graber-Sultan, S., Preische, O., Hofmann, A., Ikeuchi, T., Kasuga, K., Niimi, Y., Ishii, K., Senda, M., Cash, D., Roh, J. H., Riddle, M.C., Menard, W., Bodge, C., Surti, M., Takada, L.T., Farlow, M., Sanchez-Gonzalez, V., Orozco-Barajas, M., Renton, A.E., Esposito, B.T., Karch, C.M., Marsh, J., Fernanadez, V., Jerome, G., Herries, E., Llibre-Guerra, J., Johnson, E.C.B., Seyfried, N.T., Brooks, W.S., Bechara, J.A., Franklin, E.E., Chen, A., Chen, C., Flores, S., Hantler, N., Hornbeck, R., Jarman, S., Keefe, S., Koudelis, D., Massoumzadeh, P., McCullough, A., McKay, N., Nicklaus, J., Pulizos, C., Wang, Q., Mishall, S., Sabaredzovic, E., Deng, E., Candela, M., Smith, H., Hobbs, D., Scott, J., Xiong, C., Wang, P., Xu, X., Li, Y., Gremminger, E., Ma, Y., Bui, R., Lu, R., Martins, R., Sosa Ortiz, A.L., Daniels, A., Courtney, L., Mori, H., Supnet-Bell, P., Xu, J., Ringman, J., Barthelemy, N., Smith, J., 2023. Etiology of White matter hyperintensities in autosomal dominant and sporadic Alzheimer disease. JAMA Neurol. 80, 1353. https://doi.org/10.1001/jamaneurol.2023.3618.

Smith, S.M., 2002. Fast robust automated brain extraction. Hum. Brain Mapp. 17, 143–155. https://doi.org/10.1002/hbm.10062.

Smith, S.M., Jenkinson, M., Woolrich, M.W., Beckmann, C.F., Behrens, T.E.J., Johansen-Berg, H., Bannister, P.R., De Luca, M., Drobnjak, I., Flitney, D.E., Niazy, R.K., Saunders, J., Vickers, J., Zhang, Y., De Stefano, N., Brady, J.M., Matthews, P.M., 2004. Advances in Functional and Structural MR Image Analysis and Implementation as FSL, in: NeuroImage. https://doi.org/10.1016/j.neuroimage.2004.07.051.

Snellman, A., Ekblad, L.L., Koivumäki, M., Lindgrén, N., Tuisku, J., Perälä, M., Kallio, L., Lehtonen, R., Saunavaara, V., Saunavaara, J., Oikonen, V., Aarnio, R., Löyttyniemi, E., Parkkola, R., Karrasch, M., Zetterberg, H., Blennow, K., Rinne, J.O., 2022. ASIC-E4: interplay of Beta-amyloid, synaptic density and neuroinflammation in cognitively Normal volunteers with three levels of genetic risk for late-onset Alzheimer's disease – study protocol and baseline characteristics. Front. Neurol. 13. https://doi.org/10.3389/fneur.2022.826423.

Snellman, A., Ekblad, L.L., Tuisku, J., Koivumäki, M., Ashton, N.J., Lantero-Rodriguez, J., Karikari, T.K., Helin, S., Bucci, M., Löyttyniemi, E., Parkkola, R., Karrasch, M., Schöll, M., Zetterberg, H., Blennow, K., Rinne, J.O., 2023. APOE ε4

gene dose effect on imaging and blood biomarkers of neuroinflammation and beta-amyloid in cognitively unimpaired elderly. Alzheimer's Res Ther 15, 71. https://doi.org/10.1186/s13195-023-01209-6.

Stankoff, B., Freeman, L., Aigrot, M., Chardain, A., Dollé, F., Williams, A., Galanaud, D., Armand, L., Lehericy, S., Lubetzki, C., Zalc, B., Bottlaender, M., 2011. Imaging central nervous system myelin by positron emission tomography in multiple sclerosis using [methyl- ^{11} C]-2-(4′-methylaminophenyl)- 6-hydroxybenzothiazole. Ann. Neurol. 69, 673–680. https://doi.org/10.1002/ana.22320.

Surmak, A.J., Wong, K.-P., Cole, G.B., Hirata, K., Aabedi, A.A., Mirfendereski, O., Mirfendereski, P., Yu, A.S., Huang, S.-C., Ringman, J.M., Liebeskind, D.S., Barrio, J. R., 2020. Probing Estrogen Sulfotransferase-Mediated Inflammation with [^{11} C]-PiB in the Living Human Brain. J Alzheimer's Dis 73, 1023–1033. https://doi.org/10.3233/JAD-190559.

Tato-Fernández, C., Ekblad, L.L., Pietilä, E., Saunavaara, V., Helin, S., Parkkola, R., Zetterberg, H., Blennow, K., Rinne, J.O., Snellman, A., 2024. Cognitively healthy APOE4/4 carriers show white matter impairment associated with serum NfL and amyloid-PET. Neurobiol. Dis. 192, 106439. https://doi.org/10.1016/j.nbd.2024.106439.

Teipel, S.J., Meindl, T., Wagner, M., Stieltjes, B., Reuter, S., Hauenstein, K.-H., Filippi, M., Ernemann, U., Reiser, M.F., Hampel, H., 2010. Longitudinal changes in Fiber tract integrity in healthy aging and mild cognitive impairment: A DTI follow-up study. J Alzheimer's Dis 22, 507–522. https://doi.org/10.3233/JAD-2010-100234.

Tohgi, H., Yonezawa, H., Takahashi, S., Sato, N., Kato, E., Kudo, M., Hatano, K., Sasaki, T., 1998. Cerebral blood flow and oxygen metabolism in senile dementia of Alzheimer's type and vascular dementia with deep white matter changes. Neuroradiology 40, 131–137. https://doi.org/10.1007/s002340050553.

van der Weijden, C.W.J., Biondetti, E., Gutmann, I.W., Dijkstra, H., McKerchar, R., de Paula Faria, D., de Vries, E.F.J., Meilof, J.F., Dierckx, R.A.J.O., Prevost, V.H., Rauscher, A., 2023. Quantitative myelin imaging with MRI and PET: an overview of techniques and their validation status. Brain 146, 1243–1266. https://doi.org/10.1093/brain/awac436.

Vavasour, I.M., Vafai, N., Beauchemin, P., Kanjilal, C., Badalan, A., Shahinfard, E., Laule, C., Li, D.K., Traboulsee, A., Sossi, V., Kolind, S.H., Carruthers, R.L., 2022. A pilot study comparing myelin measurements from myelin water imaging and 11C-PIB PET in multiple sclerosis. Mult. Scler. Relat. Disord. 68, 104238. https://doi.org/10.1016/j.msard.2022.104238.

Zeydan, B., Schwarz, C.G., Przybelski, S.A., Lesnick, T.G., Kremers, W.K., Senjem, M.L., Kantarci, O.H., Min, P.H., Kemp, B.J., Jack, C.R., Kantarci, K., Lowe, V.J., 2022. Comparison of 11C-Pittsburgh compound B and 18F-Flutemetamol White matter binding in PET. J. Nucl. Med. 63, 1239–1244. https://doi.org/10.2967/jnumed.121.263281.

Zhang, M., Ni, Y., Zhou, Q., He, L., Meng, Huanyu, Gao, Y., Huang, X., Meng, Hongping, Li, P., Chen, M., Wang, D., Hu, J., Huang, Q., Li, Y., Chauveau, F., Li, B., Chen, S., 2021a. 18F-florbetapir PET/MRI for quantitatively monitoring myelin loss and recovery in patients with multiple sclerosis: A longitudinal study. EClinicalMedicine 37, 100982. https://doi.org/10.1016/j.eclinm.2021.100982.

Zhang, J., Wu, N., Wang, S., Yao, Z., Xiao, F., Lu, J., Chen, B., 2021b. Neuronal loss and microgliosis are restricted to the core of aβ deposits in mouse models of Alzheimer's disease. Aging Cell 20. https://doi.org/10.1111/acel.13380.